Central European Agroclimate over the Past 2000 Years🖉

Max C. A. Torbenson🄳,[a] Ulf Büntgen,[b,c,d,e] Jan Esper,[a] Otmar Urban,[c] Jan Balek,[c,f] Frederick Reinig,[a] Paul J. Krusic,[b] Edurne Martinez del Castillo,[a] Rudolf Brázdil,[c,d] Daniela Semerádová,[c,f] Petr Štěpánek,[c,f] Natálie Pernicová,[c,f] Tomáš Kolář,[c,g] Michal Rybníček,[c,g] Eva Koňasová,[g] Juliana Arbelaez,[c,f] and Miroslav Trnka[c,f]

[a] Department of Geography, Johannes Gutenberg University, Mainz, Germany
[b] Department of Geography, University of Cambridge, Cambridge, United Kingdom
[c] Global Change Research Institute, Czech Academy of Sciences, Brno, Czech Republic
[d] Department of Geography, Faculty of Science, Masaryk University, Brno, Czech Republic
[e] Swiss Federal Institute for Forest, Snow and Landscape Research (WSL), Birmensdorf, Switzerland
[f] Department of Agrosystems and Bioclimatology, Faculty of Agronomy, Mendel University in Brno, Brno, Czech Republic
[g] Department of Wood Science and Wood Technology, Mendel University in Brno, Brno, Czech Republic

ABSTRACT: Central Europe has experienced a sequence of unprecedented summer droughts since 2015, which had considerable effects on the functioning and productivity of natural and agricultural systems. Placing these recent extremes in a long-term context of natural climate variability is, however, constrained by the limited length of observational records. Here, we use tree-ring stable oxygen and carbon isotopes to develop annually resolved reconstructions of growing season temperature and summer moisture variability for central Europe during the past 2000 years. Both records are independently interpolated across the southern Czech Republic and northeastern Austria to produce explicit estimates of the optimum agroclimatic zones, based on modern references of climatic forcing. Historical documentation of agricultural productivity and climate variability since 1090 CE provides strong quantitative verification of our new reconstructions. Our isotope records not only contain clear expressions of the medieval (920–1000 CE) and Renaissance (early sixteenth century) droughts, but also the relative influence of temperature and moisture on hydroclimatic conditions during the first millennium (including previously reported pluvials during the early third, fifth, and seventh centuries of the Common Era). We conclude that Czech agricultural production has experienced significant extremes over the past 2000 years, which includes periods for which there are no modern analogs.

SIGNIFICANCE STATEMENT: As temperatures increase, droughts are becoming a growing concern for European agriculture. Our study allows recent extremes to be contextualized and helps to better the understanding of potential drivers. Stable carbon and oxygen isotopes in oak tree rings were analyzed to reconstruct year-to-year and longer-term changes in both temperature and moisture over central Europe and the past 2000 years. We combine these proxy-based climate reconstructions to model how well crops were growing in the past. The early fifth and the early sixteenth centuries of the Common Era were most likely characterized by extreme conditions beyond what has been experienced in recent decades. Our reconstructions of natural variability might be used as a baseline in projections of future conditions.

KEYWORDS: Europe; Paleoclimate; Tree rings; Interannual variability; Seasonal effects

---

1. Introduction

Climate extremes influence European agricultural systems in a variety of ways (Bindi and Olesen 2011). Severe droughts, with considerable negative impacts on ecosystems and with associated economic costs, have become a common feature of the twenty-first century (e.g., Bastos et al. 2020; Moravec et al. 2021). Temperature plays a significant role in summer conditions, as exemplified by the European-wide drought of 2003 and the concurrent decrease in biological productivity (Ciais et al. 2005). The consequences of water scarcity are projected to become even greater in the future (e.g., Naumann et al. 2021). In fact, the impact of climate change on agricultural yields may already have occurred (e.g., Trnka et al. 2011a, 2014). However, establishing a baseline of natural drought variability is limited by the range of our relatively short instrumental records.

Proxy records, such as tree-ring chronologies (of total or subannual ring width, density, and isotopic composition), are regularly used to reconstruct past climatic conditions (e.g., Fritts 1976; Schweingruber and Briffa 1996; Stahle et al. 2020). Soil moisture availability is often a limiting factor of tree growth, and this relationship allows for a precise and stable estimation of warm-season drought conditions experienced during the lifetime of a tree (Fritts 1976). Reconstructions of the Palmer drought severity index (PDSI; Palmer 1965) in Europe have provided insights into drought variability for the past 2000 years (e.g., Cook et al. 2015; Büntgen et al. 2021). Individual years of

low reconstructed PDSI values coincide with known droughts and agricultural failures identified in historical documents, such as 1540 for much of the European continent (Brázdil et al. 2013a; Wetter et al. 2014; Cook et al. 2015). Moreover, extended periods of continuous low (or high) PDSI values that exceed any similar length of period in the instrumental era are recorded in the reconstructions. Notable prolonged periods of drought have been identified around 550, 950, and 1500 CE, and pluvials around 200, 700, and 1100 CE for central Europe (Büntgen et al. 2021). The relative impact of temperature and precipitation on these hydroclimatic events is still unclear due to the integrated nature of PDSI (Heim 2002; van der Schrier et al. 2006).

Although soil moisture can be a good single predictor of biological productivity, the relationship between climate and yield is complex and often involves growing season length. For central Europe, summer [June–August (JJA)] precipitation minus potential evapotranspiration [hereon referred to as water balance (WB)] and the cumulative daily temperature sum for days above 10°C [hereon referred to as temperature sum (TS)] have been identified as leading climatic drivers for yields of many important crops (e.g., Trnka et al. 2011b). The two variables are negatively correlated but display significant independent variability. Instrumental records of WB and TS are limited to periods for which daily resolved observations exist, and as a result well-replicated data only start in the 1960s CE for the southern Czech Republic. Ocean–atmosphere teleconnections, such as the North Atlantic Oscillation, are thought to affect drought variability and productivity in the region (e.g., Gonsamo and Chen 2015; Mikšovský et al. 2019). The limited length of instrumental records, however, constrains our ability to place the recent central European drought extremes in a long-term context of natural hydroclimatic variability. Extended records based on proxies can help to disentangle anthropogenic from natural forcings of drought, and subsequently provide baselines for scenarios of future change.

In this paper, two annually resolved tree-ring stable isotope (TRSI) records from oak trees are used as separate predictors to reconstruct agroclimatic conditions from the first century BCE to the present day for the southern Czech Republic and northeast Austria. The reconstructions are not only skillful in their estimates of respective targets for the model calibration period, but the relationship between reconstructions also mimics that between instrumental WB and TS data. As such, the reconstructions provide new insights into the relative influence of temperature and moisture variability on agroclimatic drought over the past 2000 years. Spatial interpolation highlights changes in the suitability and productivity of important modern crop groups over time and includes extremes in moisture and temperature beyond the data range of the instrumental period.

2. Data and methods

In total, 52 meteorological stations representing observed daily precipitation and temperature data from 1961 until 2018 within the study area went through data quality control and were homogenized by means of the software ProClimDB (Štěpánek et al. 2013). The missing daily station data were then interpolated using locally weighted regression that included the influence of altitude (for more details see Štěpánek et al. 2009). A regional average was produced for each variable (see below), which serve as the targets for the TRSI-based reconstructions.

a. Selecting agroclimatologically relevant targets

The agroclimatic zoning scheme, according to Němec (2001) and as simplified by Trnka et al. (2009a), was applied in this study. This adjusted scheme considers two key agroclimatic indicators: JJA WB and the sum of daily mean temperatures above 10°C during the frost-free period of the year (TS). While TS is a good proxy of the growing season duration, summer WB provides an integrated overview of precipitation and potential evapotranspiration during the summer months, which have the highest water demand. The calculation of potential evapotranspiration was done primarily on a daily scale based on the Penman–Monteith method (Allen et al. 2005) using the SoilClim model (Hlavinka et al. 2011). Based on the daily inputs, the values of WB and TS were determined for each year during the evaluated period. The thresholds used to determine the classified types of production region of the given cadaster unit to a particular agroclimatic zone were based on the previously used values, as described by Němec (2001) and Trnka et al. (2009a, 2021). A further adjustment was necessary because neither the set of original agroclimatic zones derived for the climate of 1931–60 by Němec (2001) nor the updated version by Trnka et al. (2021) for climate of 1961–2020 would cover all conditions encountered during the reconstruction period. Therefore, two new regions ("grape vine" and "very hot and very dry" production regions) were added to account for the warmer and drier part of the classification scheme. Additionally, the "cereal growing" and "forage growing" production regions were each divided into two subcategories based on TS to better capture nuances of cooler periods (see Table S1 in the online supplemental material).

b. Proxy data, model calibration, and verification

Tree-ring stable isotopes from 147 cores and discs of living, subfossil, and archaeological material from central Europe were used, with an even sample distribution across the entire period studied. Six samples at a minimum make up the chronology average at any given year of the TRSI records. In total, over 27 000 nonpooled measurements from the latewood alpha cellulose make up the proxies. These data have previously been described in detail by Büntgen et al. (2021). Because neither the $\delta^{13}C$ nor the $\delta^{18}O$ data contain significant age-related trend (Büntgen et al. 2020; Urban et al. 2021), detrending was therefore not considered necessary prior to use in the reconstruction calibration (Esper et al. 2010). Here, the inverse median for $\delta^{18}O$ and $\delta^{13}C$ were treated as separate predictors. Each TRSI was entered into a separate simple regression model with JJA water balance ($\delta^{13}C$) and temperature sum ($\delta^{18}O$) as target predictands. Model calibrations were performed on the full period shared between predictor and targets (1961–2018). Prediction intervals were calculated for each

calibration and were considered uncertainty ranges of the respective reconstruction (Olive 2007).

The relation between mean temperature (for TS) and precipitation total (for WB) (CRU; Harris et al. 2020) for the temporally closest combination of months was calculated through simple correlation over the calibration period (1961–2018). The identified CRU variable for respective target was used as verification for the precalibration period. The WB estimates were also correlated with gridded JJA precipitation reconstructions based on historical documents and other proxy records (Pauling et al. 2006) for the period 1500–1900 CE. Similarly, the TS estimates were compared with the Luterbacher et al. (2016) gridded reconstructions of JJA temperature for the same period.

Brázdil et al. (2013a) identified agricultural failures and droughts in the Czech Republic for the period 1090–1499 CE based on documentary sources (e.g., annals, chronicles, municipal books of accounts, letters, and epigraphic materials). For example, the Old Czech Annals reported great heat, no rain for 3.5 months, forest fires, dried-up rivers and brooks, and loss of crops due to drought in 1473. Of the 36 events identified in documentary evidence, 29 were used for comparison with the reconstructions (Table S2 in the online supplemental material). Events that occurred prior to or after the summer season and did not include one of the June, July, or August months were excluded from the comparison (a total of 7 of the 36 events). A Monte Carlo (bootstrap) approach (Mooney and Duval 1993) was used to estimate the two-tailed confidence intervals (CI) for anomalies of the event years by Brázdil et al. (2013a). The mean of reconstructed WB and TS for 29 randomly resampled years (between 1090 and 1499 CE) was calculated 10 000 times, and a normal distribution was fitted to the data. Qualitative comparisons with documentary studies of climatic and agricultural extremes were also performed.

c. Spatial interpolation and agricultural yield analysis

To produce a climatological series representing past agroclimatic conditions for the study area, we used an approach applied for the agroclimatic zone reconstruction by Trnka et al. (2011b). The approach is based on the "delta method," i.e., shifting the WB and TS values at the given site for the given period by the offset derived from comparison of the period WB and TS reconstructed time series (section 2b) from the baseline (1961–2018). The values of both indices were perturbed (through the delta method) at the site of the individual stations. In the next step, the median values of both indices for each period were interpolated from those 52 meteorological stations using locally weighted regression that included the influence of altitude using a terrain model with 100-m resolution (Farr et al. 2007) and finally aggregated to the level of individual cadasters units. The interpolation errors of both WB and TS were similar for all periods and should not influence the overall results of the study. To verify the performance of the method, all calculations for 1961–2018 were performed with observed as well as estimated WB and TS values. The values of WB and TS at 52 meteorological stations and those interpolated to individual cadaster units are not significantly

different, and the production region classification agrees in more than 98% of cases.

3. Results

The δ^{18}O series is statistically significantly correlated with both TS ($r = -0.690$; $p < 0.01$) and WB ($r = 0.583$; $p < 0.01$) for the 1961–2018 calibration period. Because the two instrumental targets are weakly correlated ($r = -0.339$; $p < 0.01$) for the calibration period, this dual signal in the proxy record may stem, in part, from the interrelationship of WB and TS. To limit exaggerated correlations between the reconstructions, δ^{18}O was omitted from the WB predictor pool and only used as a predictor for its strongest relationship (TS). An alternative water balance calibration model with both δ^{18}O and δ^{13}C was produced for comparison. Conversely, the δ^{13}C series does not show any statistically significant correlation with TS ($r = 0.016$; $p > 0.10$).

a. Calibration statistics and reconstruction estimates

The regression model using δ^{13}C as a predictor explains 31.3% of the variance in the regional WB average for the 1961–2018 calibration period. For TS, the model using δ^{18}O explains 48.7%. The full-period reconstructions extend the instrumental record back by 2035 years (Fig. 1), with significant variability in the preinstrumental period. Notable examples of multidecadal to centennial periods of anomalies include continuous dry conditions for 920–1050 CE, wet conditions for 150–250 CE (Fig. 1a), and low growing season temperature sums for 350–420 and 650–750 CE (Fig. 1b).

The two reconstructions suggest a trend toward drier and warmer climate (Fig. 1), which is expected as there is a significant decreasing trend in the previous PDSI reconstruction (Büntgen et al. 2021). Since 1900 CE, the positive trend is stronger in TS, but for the 1700–present-day period the trend (negative) is stronger in WB. Over the full period of reconstruction (75 BCE–2018 CE), adjusted Mann–Kendall tests (Kendall 1975; Hamed and Rao 1998) indicate statistically significant trends with the same sign [i.e., positive for TS ($p < 0.01$) and negative for WB ($p < 0.01$)]. The linear trends explain 12.1% and 6.2% of the variance for WB and TS, respectively, over the full reconstruction period (Fig. 1).

b. Verification of estimates

Correlations between WB and gridded JJA precipitation for prior to 1960 are positive over the region in consideration. Although some loss of agreement is expected (due to different variable types), comparison with the CRU data allows for a general insight to the temporal stability of the temperature and hydroclimate signals that underpin the reconstructions. Correlations are weaker than those for the calibration period, and furthermore, the highest agreement can be found in southern Poland ($r > 0.45$; Fig. 2a). Correlations between TS and gridded JJA mean temperature for the same period (1901–60) reveal weak but positive correlations over the Czech Republic and beyond (Fig. 2b). The spatial homogeneity and extent of the correlation is expected because of the greater spatial homogeneity of temperature variables.
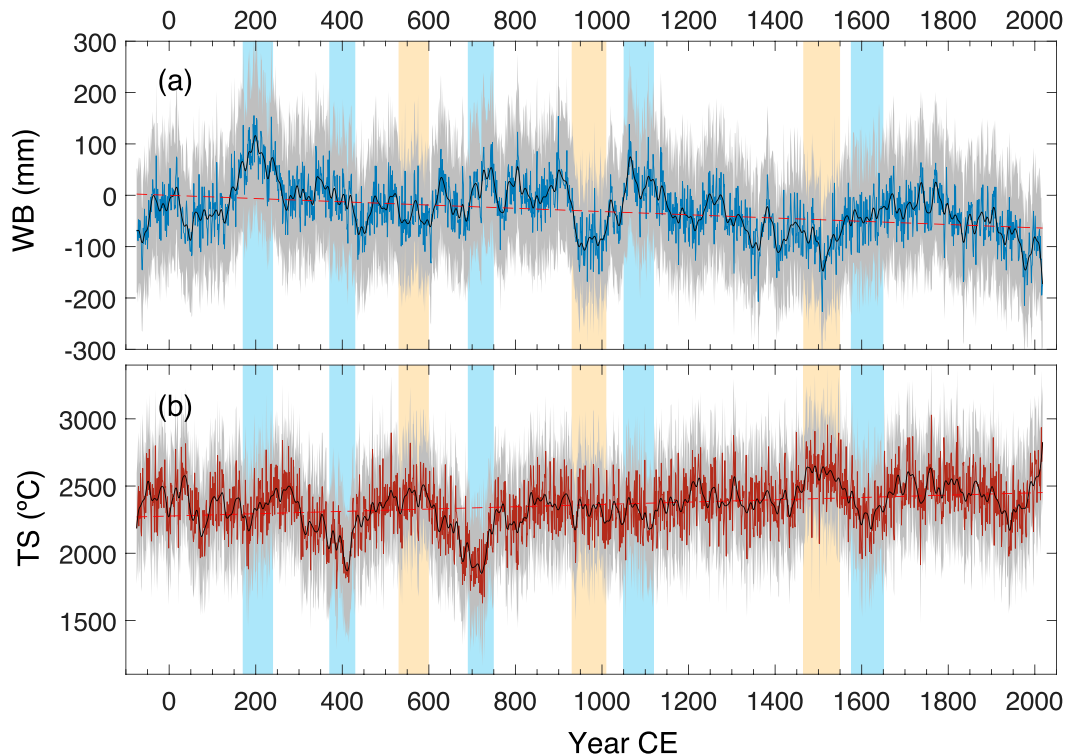
FIG. 1. Reconstructions of (a) water balance and (b) temperature sum from 75 BCE to 2018 CE based on oak TRSI from central Europe. Blue/red lines represent the interannual variations, with the shaded gray area being the 95% prediction interval of the calibration model. A smoothing spline (black) was fitted to each reconstruction to accentuate low-frequency variability of the time series. Light-blue and yellow periods respectively highlight previously described pluvials and droughts, and the red dashed line represents statistically significant long-term linear trends [$y = -0.031\,61x + 2.317$, with $r^2 = 0.1210$, in (a), and $y = 0.086\,47x + 2270$, with $r^2 = 0.0621$, in (b)].

Similar correlations are also recorded for gridded reconstructions of temperature and precipitation based on sources independent of the Czech TRSI series (Figs. 2c,d), suggesting that the underlying signal was stable not only for the twentieth century precalibration period but for the past 500 years. As expected from these correlations, many pre-1900 years of extreme conditions known from the documentary evidence are present in the reconstructions. For example, Brázdil et al. (2019) listed 16 negative anomalies of JJA Z index (an estimate of atmospheric moisture close to the water balance reconstruction target; Palmer 1965; Heim 2002) for 1501–1803 in the Czech Lands. All years except two (1631 and 1666) fall below the 30th percentile (of the entire reconstruction period), with the most extreme years also standing out in the water balance reconstruction (e.g., 1540, 1556, 1590, 1740). Known multiyear droughts are also present, including that of 1506–07 (Kiss 2020), for which the estimates of available moisture rank in the second and first percentiles, respectively (of the entire reconstruction period).

For the 29 drought events prior to 1500 CE used for the Monte Carlo simulation, there appears to be clear associations with both the available moisture (CI < 0.001) and temperature sum (CI < 0.05) reconstructions (Fig. 3). It is therefore also expected that many of the individual years for

which we have documentary evidence stand out in the reconstructions, especially so for the available moisture estimates. This is the case for events that may have been part of spatially extensive extremes. Anomalies of dry conditions include 1473 (Camenisch et al. 2020), which was also a part of the Brázdil et al. (2013a) list, but also 1361 and 1494. These three years have been linked to droughts in Hungary that occurred in the following years (Kiss and Nikolić 2015), not dissimilar to the 1506–07 drought at the start of the century that followed (Kiss 2020).

The year 1361 also displays one of the five lowest estimated PDSI values of the 1000–1900 CE for the territory of the Czech Republic in the Old World Drought Atlas (OWDA; Cook et al. 2015). The OWDA is also produced from tree-ring-based variables; however, no isotope series were used, and our new estimates can therefore be considered as independent. Statistically significant correlations between the PDSI reconstruction from the same predictors used here and the local OWDA grid points have been recorded ($r = 0.34$; $p < 0.001$; Büntgen et al. 2021). Other extreme years in the first half of the most recent millennium during which the OWDA records less-than-first-percentile values include 1177 and 1305–06 CE (the driest years in over 300 years in the WB reconstruction).
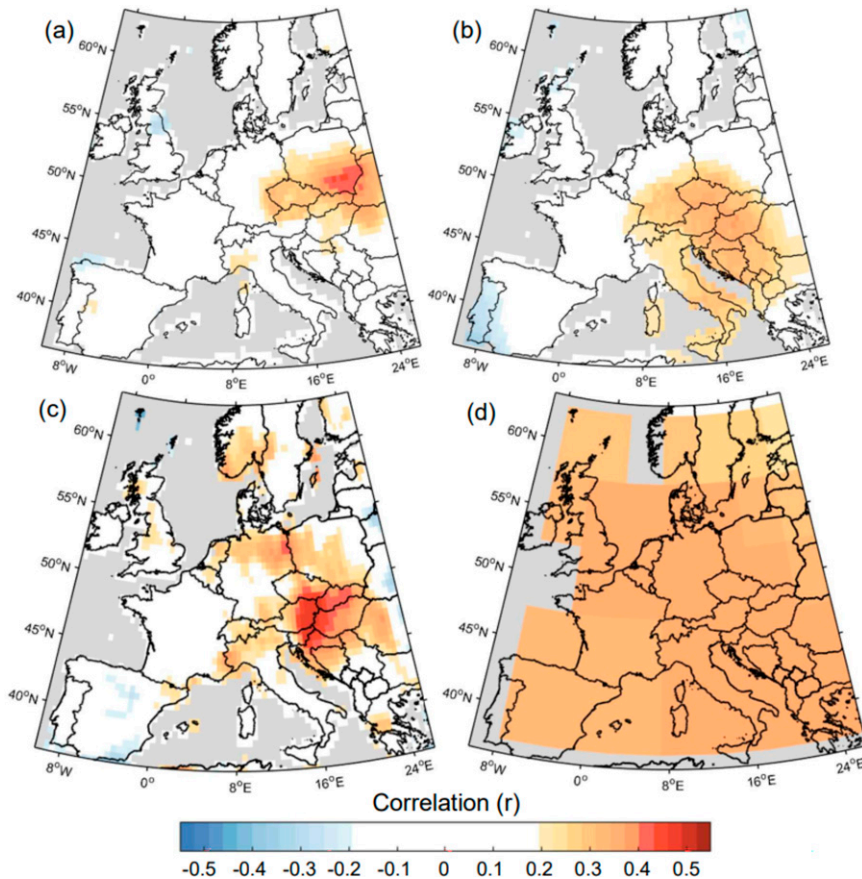
FIG. 2. Correlation between (a) reconstructed JJA water balance estimates presented here and CRU JJA precipitation totals and (b) reconstructed temperature sum estimates and CRU JJA mean temperature for the period 1901–60 CE. (c) As in (a), but correlated with gridded JJA precipitation reconstructions (Pauling et al. 2006) for the period 1500–1900. (d) As in (b), but with the JJA temperature reconstruction by Luterbacher et al. (2016) for 1500–1900.

Documentary evidence of temperature fluctuations tends to be biased toward cold events, and there are numerous examples of "years without a summer" from central Europe (Pfister and Wanner 2021). Examples of such years include 1144 (14th and 20th percentile of the 1000–1499 CE and the entire reconstruction, respectively) and 1151 (2nd and 6th percentile). Three consecutive years of cold summers are also present in regional documentary accounts (Pfister and Wanner 2021): 1195 (77th and 75th percentile), 1196 (3rd and 9th percentile), and 1197 (20th and 25th percentile). In the TS reconstruction, 1335 stands out as the second coldest summer between 1090 CE and present day. Despite the scarcity of documentary records, harsh conditions in specific years prior to 1090 CE were documented. The year 1042, described as a year without a summer from France to western Poland (Alexandre 1987), stands out in the TS reconstruction and falls far below the mean in this year (<3rd and 8th percentiles).

c. Relationship between reconstruction estimates

The two reconstructions are correlated at $r = -0.347$ ($p < 0.01$) for the calibration period (1961–2018), similar in

magnitude to the instrumental data ($r = -0.339$; $p < 0.01$). The relationship between WB and TS for the full period of reconstruction (75 BCE–2018 CE) is also of a similar level ($r = -0.307$; $p < 0.0001$; Fig. 4a). The alternate WB reconstruction, using both $\delta^{13}C$ and $\delta^{18}O$ as a combined predictor (like the approach taken by Büntgen et al. 2021), produces higher correlations ($r = -0.880$) between WB and TS estimates for the calibration period and the difference in correlation is statistically significant ($p < 0.001$ based on Fisher's z transformation; Fisher 1921). Although this combined predictor reconstruction displays stronger calibration statistics, the exaggerated positive correlation between TS and the resulting WB estimates leaves little independent variance and is unlikely to represent the true nature of the temperature–hydroclimatic relationship in the region. The TS is higher than the long-term mean for most extreme negative WB years; however, this is not the case for years of the positive WB values (Table 1).

Not unlike the dry values, years with high TS estimates co-occur with drier conditions in the WB reconstruction (Table 2). Of the 10 hottest years of the past 2000 years, all are estimated
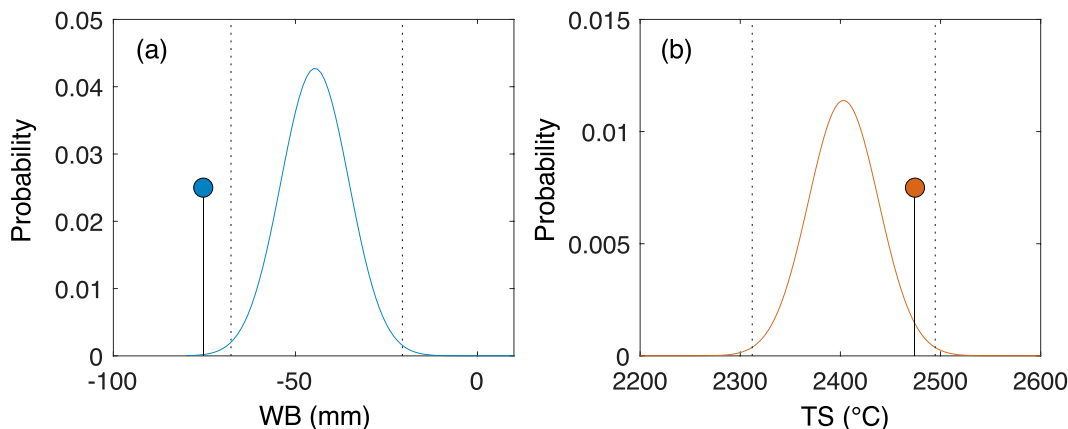
FIG. 3. The mean (a) water balance and (b) temperature sum estimates for 29 drought events identified in Czech documentary data (Brázdil et al. 2013a) for the period 1090–1499, plotted as filled circles, with distributions of a Monte Carlo simulation for comparison. The dotted lines indicate the 0.01 confidence intervals.

to have been below the long-term mean in WB. The relationship also holds stronger for the cold extremes, for which 8 of the 10 coldest years are suggested to have been wetter than the mean (with 7 being in the 85th percentile or lower). These results suggest that despite relatively weak overall correlation between WB and TS (the common variance explaining ~10% of the variability), the relationship may be stronger during years of extreme conditions.

Some years, and extended periods of years, do not adhere to this negative relationship between WB and TS. The year 236 CE ranks as the third wettest year of the Common Era (Table 1) but also displays high temperature sums. It does not appear to be an isolated event, as the late second and early third centuries CE stand out. The periods 184–241 and 365–422 CE display diametrically opposite values of WB and TS (Fig. 4c): 184–241 is characterized by relatively warm and wet estimates while 365–422 CE displays cool and dry conditions, not dissimilar to the early medieval pluvial (Fig. 4f; Büntgen et al. 2021). In the Büntgen et al. (2021) PDSI reconstruction, these two periods appear very similar to each other with non-significant differences in mean and distribution (Figs. 4d,e). Unlike the calibration period, during which reconstructed values fall on both sides of the long-term regression line, these three first millennium periods (184–241, 365–422, and 670–727) are skewed toward conditions that deviate from the negative relationship.

4. Discussion

The oak TRSI series analyzed here represent an important dataset for the understanding of long-term climate variability in central Europe (Büntgen 2022), in part due to the relatively low correlation between δ^{18}O and δ^{13}C (e.g., Saurer et al. 1997) and the distinct climate signals within the respective series. It is, however, important to acknowledge the limitations and uncertainties associated with both proxy data and subsequent reconstructions. A lack of age-related trend in the individual series used to produce the stable oxygen and carbon chronologies has been shown (Büntgen et al. 2020) but certain

factors that influence TRSI variability, including surrounding environment and the height (on the tree) from which the samples were taken, are unknown for some of the older material (Gessler et al. 2014). The reconstructions leave considerable amounts of variance in the targets unexplained, as evident in the wide prediction intervals (Fig. 1). Nonetheless, precalibration estimates from our conservative reconstruction model can be qualitatively and quantitatively verified against known events over the past millennium in the long documentary record of extreme cold, warm, wet, and dry conditions from the Czech Republic.

a. Climate signals and reconstruction targets

Climatic signals in TRSI series have shown to be diverse across space and species boundaries (e.g., Treydte et al. 2007; Leavitt 2010; Hartl-Meier et al. 2015; Nguyen et al. 2021). Variability in tree-ring δ^{13}C records from higher latitude or altitude sites has often been connected to temperature variables (e.g., Treydte et al. 2009; Liu et al. 2014). However, this relationship may be partly a result of intercorrelation with relative humidity (McCarroll and Loader 2004; Esper et al. 2018). At more temperate sites, and where moisture availability is not a significant factor, vapor pressure deficits appear to impact δ^{13}C in oaks through stomatal conductance (Baldocchi and Bowling 2003). Precipitation and vapor pressure deficit have been linked to stable carbon isotope variability in other white oak species (Voelker et al. 2014), and *Q. robur* trees (as used here) from nearby Hungary display similar relationships with local precipitation variability (Kern et al. 2013). Recently, Churakova-Sidorova et al. (2022) recorded strong hydroclimatic signals in δ^{13}C and temperature signals in δ^{18}O of *Larix sibirica*—the same predictor-target and sign combinations as recorded by the oak TRSIs analyzed here. Ultimately, climatic drivers of TRSI variability are complex and likely include multiple coexisting influences (McCarroll and Loader 2004; Esper et al. 2018). Signals should be analyzed on a site-to-site basis, but TRSI in the Czech oaks appear to respond to both temperature and hydroclimate.
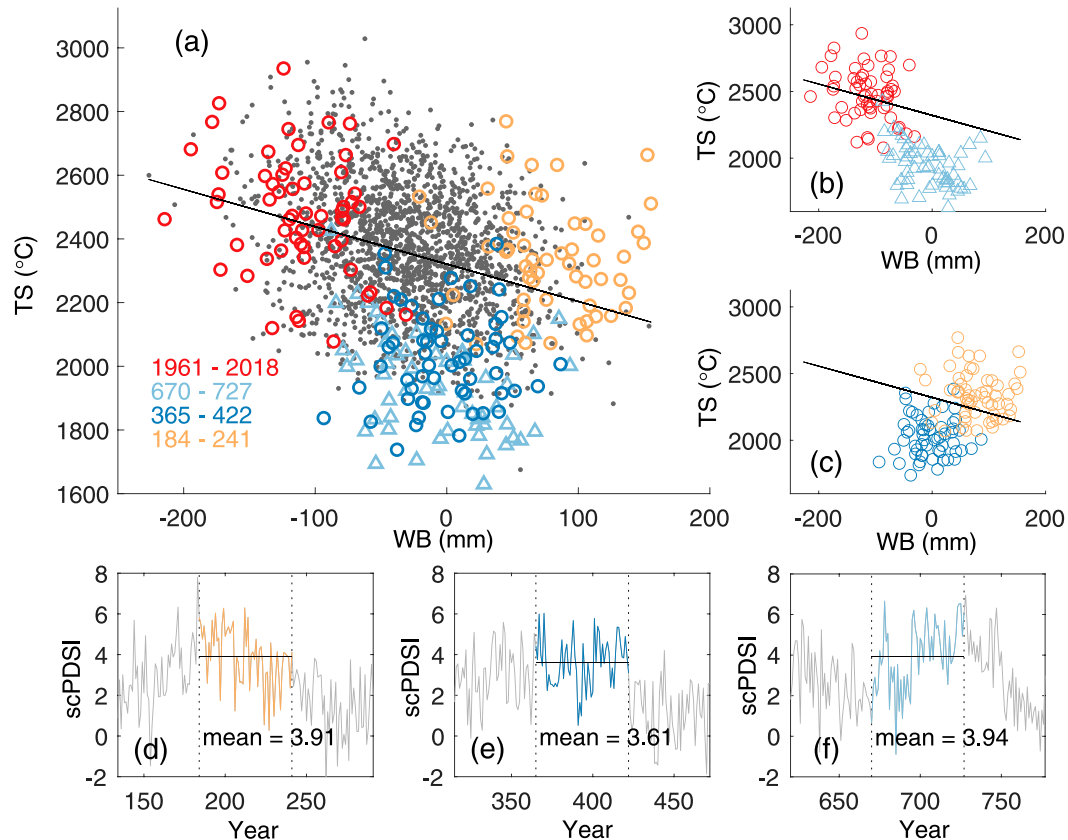
FIG. 4. (a) Relationship between reconstructed water balance and temperature sum estimates from 75 BCE to 2018 CE. Three noteworthy periods, and the calibration period, are plotted in color. (b) Comparison between the calibration period and early medieval pluvial estimates, and (c) comparison between the Late Roman pluvial and the period around the Great Migration. (d)–(f) Estimates of PDSI from Büntgen et al. (2021) for the three first-millennium-CE periods.

We suggest that the previous PDSI reconstruction is possible because of two separate responses that affect soil moisture in the same direction: 1) precipitation with a negative influence on $\delta^{13}C$ and 2) temperature having a positive impact on $\delta^{18}O$ isotope variability. Consequently, years of extremes in the PDSI are likely to have strong opposite magnitudes in the isotope series. The robustness of such a reconstruction thus rests on an assumption that the two variables are relatively

even in their impact on PDSI, and that the relationship during the calibration period has been stable throughout the past 2000 years. Büntgen et al. (2021) noted significantly lower correlations between the $\delta^{13}C$ and PDSI after 1960 and attributed this decline to industrial pollution. However, the separation of signals in the two stable isotope records offers an alternative explanation: the role of temperature in drought conditions has increased over recent decades, leading to a

TABLE 1. The 10 driest and wettest years in the water balance reconstruction and the percentile of reconstructed temperature sum (TS) for the corresponding year.

Rank (dry)	Year CE	Percentile TS	Rank (wet)	Year CE	Percentile TS
1	1509	88	1	196	78
2	1976	69	2	899	14
3	1361	77	3	236	94
4	2016	95	4	202	56
5	1508	97	5	203	63
6	2017	98	6	194	27
7	1982	78	7	1063	70
8	1983	82	8	171	19
9	2018	99	9	199	21
10	1977	39	10	198	47

TABLE 2. As in Table 1, but with the 10 hottest and coldest years of the TS reconstruction, with WB percentiles of the corresponding year indicated.

Rank (hot)	Year CE	Percentile WB	Rank (cold)	Year CE	Percentile WB
1	1761	27	1	724	85
2	1521	7	2	728	94
3	1822	19	3	721	33
4	2015	4	4	718	56
5	1492	2	5	696	86
6	1449	21	6	387	45
7	513	37	7	704	91
8	1547	9	8	678	94
9	1530	3	9	707	66
10	1304	10	10	723	92

precipitation-sensitive proxy (δ^{13}C) to lose shared variance with PDSI during the same time.

b. Extreme events and periods in the preinstrumental era

The reconstructions of WB and TS indicate numerous examples and extended periods of values that fall outside the range of the 58-yr instrumental calibration period. Significant trends are noted for both full reconstructions, with a general shift toward warmer and drier conditions, although these trends appear marginally weaker than that of the previous PDSI reconstruction. Because of the daily meteorological data needed to produce the reconstruction targets, the calibration period leaves out more than half of the twentieth century. Several years in the WB and TS estimates between 1900 and 1960 coincide with well-known climatic events (Rybníček et al. 2021). For example, the coldest 3-yr stretch since the early ninth century CE in the TS reconstruction is recorded for 1940–42, a period of global climatic anomalies that include lower European temperatures (Brönnimann 2005). The early 1930s were marked by pronounced droughts, culminating in 1934 (Trnka et al. 2009b). The WB reconstruction displays continuous low moisture from 1928 with the lowest value (less than second percentile) recorded for 1934. Central Europe, and the Czech Republic in particular, has a long tradition of high-quality documentary evidence of past environmental variability. These include reports of weather and related phenomena (e.g., Brázdil et al. 2022) and records of grape harvest (Možný et al. 2016) or cereal harvest (e.g., Možný et al. 2012). This myriad of documents allows for a rare opportunity for quantitatively testing the reconstruction estimates against independent data for almost a millennium prior to the twentieth century. The results of the Monte Carlo simulation indicate a strong relationship between both reconstructions and extreme single-year drought in the study region back to 1090 CE.

Longer fluctuations, that extend beyond that of the interannual and decadal, have been recorded in documentary and proxy records. One of these is the 1516–59 warm period indicated by Možný et al. (2016) using grape harvest dates, which also stands out in a similar spring and summer temperature reconstructions from the wider central European region (Možný et al. 2012; Camenisch et al. 2016). This period overlaps with the warmest 50 years of the TS reconstruction (Fig. 1b).

Although the TS reconstruction indicates that the period was an extension of an equally warm end of the fifteenth century, a full comparison is not possible because of the start date of the yield-based reconstructions (1499 or 1501). Conversely, the lower temperatures suggested for the late sixteenth century coincide with poor harvests and extensive problems for the wine industry in the region (Brázdil et al. 2013b). The decline in the TS reconstruction persists well into the 1600s, making the seventeenth century the coldest century of the second millennium CE. The severity of this cold spell has also been suggested by other robust summer temperature reconstructions from neighboring regions (e.g., Büntgen et al. 2006, 2011).

All anomalies suggested by the WB and TS reconstructions do not align with previous studies. Perhaps the most notable example is 1345—for which OWDA indicates wet conditions. Here, the TS reconstruction records just above the mean, but WB is below the 1st percentile. The WB reconstruction shows that 1345 was the start of an extended period of moisture depletion—similar, but perhaps more extreme, to that of the early 1930s. Conversely, the OWDA indicates severe drought conditions in 1384 but the WB reconstruction suggests very wet atmospheric conditions. The TS for 1384 is, however, the highest reconstructed value of the surrounding 150 years and could potentially explain part of the drought conditions recorded by total ring-width records (e.g., the OWDA). Although unlikely to account for all differences with existing records, the independent variability of the two reconstructions (and the relationship between the two) may offer new perspectives on preinstrumental conditions.

c. The relationship between growing season temperatures and water balance

The exceptionally strong statistics of the Büntgen et al. (2021) PDSI reconstruction are undoubtedly reflective of a robust signal in the TRSI, and the new WB and TS reconstructions are not meant to replace the previous estimates of soil. In fact, the PDSI reconstruction is strongly correlated with both the WB ($r = 0.836$; $p < 0.001$) and TS ($r = -0.776$; $p < 0.001$) estimates presented here. Nonetheless, the WB and TS reconstructions provide alternative perspectives on climate variability, especially as it pertains to agriculture, over the territory of the Czech Republic and beyond for the past 2000 years.

The correlation between the predictors for the calibration period is not significantly different from that of the instrumental data, and the magnitude of correlation is similar for the entire period. We, therefore, argue that the shared variance between predictor and predictand is primarily related to each respective signal, and that the "noise" (or unexplained variance in the calibration model) can be assumed to not bias the relationship between reconstructions. Over the entire reconstruction period, the magnitude of correlation is like that of the calibration period (for both reconstructed and instrumental data) but there are numerous examples of individual years that deviate from this weak negative relationship, as well as several multidecadal fluctuations.

Separating these two factors may reveal climatic events that are not evident from PDSI alone. An example of such an event is the years 1770–71. The reconstructed TSs for the two years are near the long-term mean; however, WB estimates fall in the 88th and 95th percentile (of the full reconstruction), respectively. The high anomalies in WB coincide with poor harvests in the historical record attributed to extremely wet conditions (Pfister and Brázdil 2006), and the low crop yields may even have played a role in societal upheaval in 1770–72, called "hungry years" in the Czech Lands (Brázdil et al. 2001). Comparable to other preinstrumental events, these anomalies appear to have occurred within a spatially homogeneous period in central Europe, evident by the long-term high precipitation indicated by a spring–summer precipitation reconstruction from southern Germany (Wilson et al. 2005).

A similar period is recorded in the WB reconstruction for the mid-eleventh century CE. Between 1060 and 1074 CE, 15 consecutive years above the 75th percentile (of the entire reconstruction period) are recorded. Unlike other wet stretches indicated over the past millennia, temperature sums are estimated to be near or above the mean (mean TS for 1060–74 is equal to the 55th percentile of the entire period). The PDSI reconstruction indicates very wet conditions for this period but that other long-term fluctuations for which this is not as clear exist—most notably during the first millennium of the Common Era (Fig. 4).

The 184–241 CE period stands out as some of the wettest years, but in the context of the first millennium, these years were also relatively warm. Few, if any, documentary records can corroborate this information, but these decades could provide a basis for future scenarios that are beyond what has been measured by instruments, not only in terms of absolute values but also for the relationship between variables. These years of relatively warm but wet conditions have been rare in terms of long-term climate variability but represent conditions that are not present in the short instrumental record. This holds especially true for multidecadal or subcentennial length periods. It is also likely that, if the signals present in the TRSI are what we suggest, some high first millennium PDSI values of Büntgen et al. (2021) are driven by low temperatures.

d. Changes in agricultural suitability over the past 2000 years

The influence of past climate variability on agricultural productivity, and subsequent societal responses, is a well-studied relationship (e.g., Esper et al. 2017; Tello et al. 2017). Soil moisture estimates, such as PDSI, are not always the strongest climatic variable documenting historic European agricultural yields (Ljungqvist et al. 2022). For the modern period, the two reconstructed targets (WB and TS) represent strong explanatory variables for agricultural productivity in our area of study (Trnka et al. 2011b). A clear gradient across Moravia (the eastern part of the Czech Republic) and northeast Austria from the northwest to the southeast is evident in optimum agroclimatic region for the calibration period (Fig. 5e).

The modeled estimates of production prior to 1961 display several periods of similar conditions to that of the calibration period. The lower TSs for much of the reconstruction period (Fig. 1b) are interspersed with phases of warmer and drier conditions, such as the late fifteenth and early sixteenth centuries CE during which the production regions in the eastern part of the study area were less optimum for sugar beet and maize than the recent 58 years (Figs. 5c–e). This period, and others like it, represent scenarios of agroclimatic conditions within the range of natural variability that are likely to occur in the future but exacerbated by anthropogenic forcing.

Current agroclimatic concerns for the region are linked to drought variability and high temperatures, but in the past cool and wet conditions may have been equally troublesome for agricultural productivity (e.g., 1770–71 CE). Similar periods have been noted in older documentary sources, including extensive flooding and famine in the early 1280s and flooding during the 1314–16 disease outbreak in Bohemian livestock (Brázdil et al. 2018). The latter may have been part of early stages of the "Great European Famine" (Jordan 1996). The WB reconstruction displays some of the highest multiyear values in the past millennium for 1281–83 and 1314–15 CE. The two-dimensional nature of the reconstructions presented here thus allow for a better understanding of the climatic factors that have dictated the suitability of farming in the past. The optimum agricultural regions differ for more than half of the study area between 184–241 and 365–422 CE (Figs. 5a,b), whereas these periods would not have differed dramatically if the results were produced using a single PDSI predictor (Figs. 4d,e). The modeled productivity suggests that the warmer period (184–241 CE) produced more favorable conditions across most of western and central Moravia, whereas one-third of our study region was unsuitable for any agricultural yield during the latter period (365–422 CE).

Future studies should aim to combine archaeological evidence, paleobotanic and paleoecological data, documentary sources, and paleoclimatic estimates to produce more robust hypotheses on how climate-induced environmental changes may have shaped past agriculture and the resulting societal responses. The WB and TS reconstructions presented here cover periods of conditions not recorded by modern observations and offer baselines for future scenarios. The results also represent robust estimates of the climatic signals embedded in the stable isotope variability of oaks from central Europe. The development and extension of longer records can rely on the analyses performed here. As such, the potential for exploring climatic forcing on sustenance for the earliest Neolithic communities in central Europe is within closer reach than ever before.
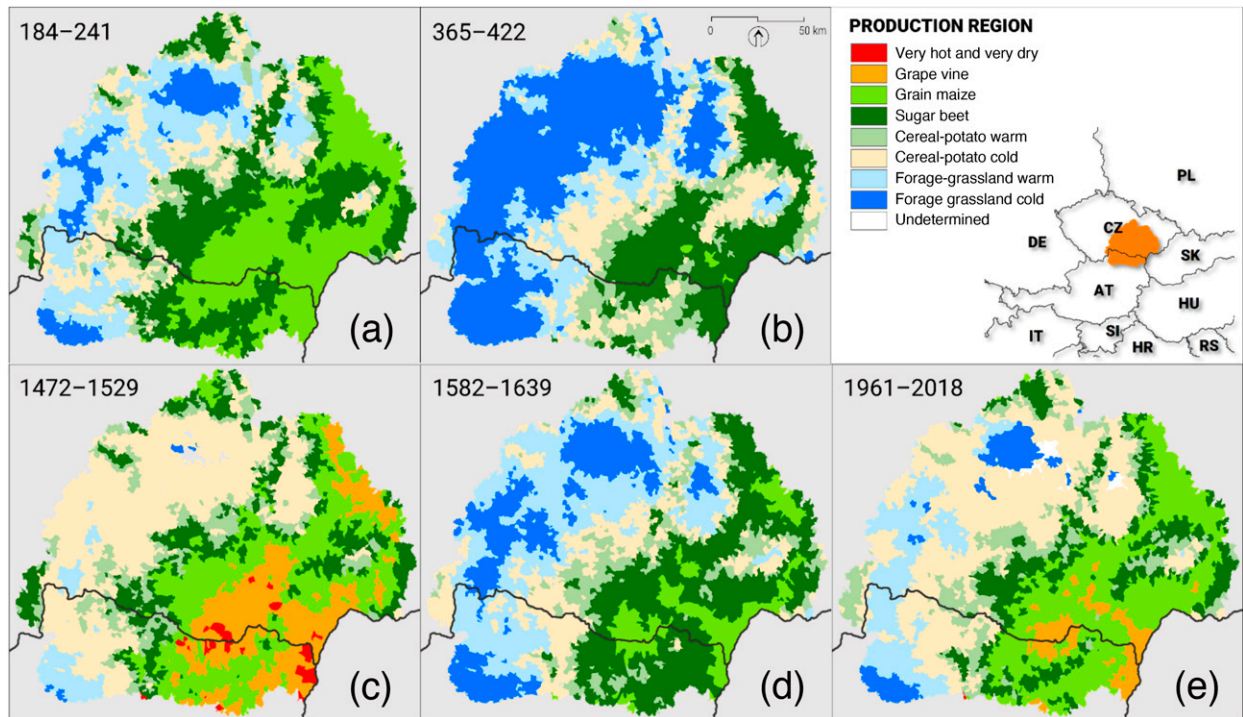
FIG. 5. Reconstructed production regions for five selected 58-yr periods of extremes highlighted by the WB and TS reconstructions in Moravia and northeast Austria. The sugar beet production region is considered to be most productive in terms of agroclimatic conditions, whereas grain maize, grape vine, and very hot and very dry regions are warmer, albeit too dry to achieve maximum productivity. Conversely, cereal–potato and forage–grassland regions tend to be too cool (and in some instances too wet) for optimum productivity.

5. Conclusions

Stable carbon and oxygen isotope variability in tree rings from Czech oaks relate to different climatic variables. These relationships allow for the deconstruction of PDSI estimates previously derived from the combined isotope data into separate temperature and precipitation-related components. The WB and TS reconstructions verify strongly for the past 1000 years and display more extreme annual and decadal values prior to the calibration period than what has been observed during the past 60 years. Many of such years align with societal upheaval indicated by documentary evidence. However, the statistically significant trends present in the reconstructions also suggest a continuous shift toward warmer and drier conditions. The two reconstructions allow for the modeling of optimal agroclimatic zones across Moravia and northeast Austria for the past two millennia and indicate large changes in the spatial suitability of today's most important agricultural crops. These estimates provide a baseline for the natural variability of agroclimatic drivers in the region and may also offer a more nuanced picture of the conditions faced by prehistoric agricultural communities.

REFERENCES

Alexandre, P., 1987: *Le climat en Europe au Moyen Age: Contribution à l'histoire des variations climatiques de 1000 à 1425, d'après les sources narratives de l'Europe occidentale.* Ecole des hautes études en Sciences Sociales, 827 pp.

Allen, R. G., I. A. Walter, R. L. Elliot, T. A. Howell, D. Itenfisu, M. E. Jensen, and R. Snyder, 2005: *The ASCE Standardized Reference Evapotranspiration Equation.* American Society of Civil Engineers, 216 pp.

Baldocchi, D. D., and D. R. Bowling, 2003: Modelling the discrimination of $^{13}CO_2$ above and within a temperate broad-leaved

forest canopy on hourly to seasonal time scales. *Plant Cell Environ.*, **26**, 231–244, https://doi.org/10.1046/j.1365-3040.2003.00953.x.

Bastos, A., and Coauthors, 2020: Impacts of extreme summers on European ecosystems: A comparative analysis of 2003, 2010, and 2018. *Philos. Trans. Roy. Soc.*, **A375**, 20190507, https://doi.org/10.1098/rstb.2019.0507.

Bindi, M., and J. E. Olesen, 2011: The responses of agriculture in Europe to climate change. *Reg. Environ. Change*, **11**, 151–158, https://doi.org/10.1007/s10113-010-0173-x.

Brázdil, R., H. Valášek, J. Luterbacher, and J. Macková, 2001: Die Hungerjahre 1770–1772 in den Bömischen Ländern: Verlauf, meteorologische Ursachen und Auswirkunge. *Österreichische Z. Geschichtswissenschaften*, **2**, 44–78, https://doi.org/10.25365/oezg-2001-12-2-3.

——, P. Dobrovolný, M. Trnka, O. Kotyza, L. Řezníčková, H. Valášek, P. Zahradníček, and P. Štěpánek, 2013a: Droughts in the Czech Lands, 1090–2012 AD. *Climate Past*, **9**, 1985–2002, https://doi.org/10.5194/cp-9-1985-2013.

——, O. Kotyza, P. Dobrovolný, L. Řezníčková, and H. Valášek, 2013b: *History of Weather and Climate in the Czech Lands X: Climate of the Sixteenth Century in the Czech Lands*. 1st ed. Masaryk University, 285 pp.

——, ——, and M. Bauch, 2018: Climate and famines in the Czech Lands prior to AD 1500: Possible interconnections in a European context. *Famines During the 'Little Ice Age' (1300–1800)*, D. Collet and M. Schuh, Eds., Springer, 91–114, https://doi.org/10.1007/978-3-319-54337-6_5.

——, P. Dobrovolný, M. Trnka, L. Řezníčková, L. Dolák, and O. Kotyza, 2019: Extreme droughts and human responses to them: The Czech Lands in the pre-instrumental period. *Climate Past*, **15**, 1–24, https://doi.org/10.5194/cp-15-1-2019.

——, ——, J. Mikšovský, P. Pišoft, M. Trnka, M. Možný, and J. Balek, 2022: Documentary-based climate reconstructions in the Czech Lands 1501–2020 CE and their European context. *Climate Past*, **18**, 935–959, https://doi.org/10.5194/cp-18-935-2022.

Brönnimann, S., 2005: The global climate anomaly 1940–1942. *Weather*, **60**, 336–342, https://doi.org/10.1256/wea.248.04.

Büntgen, U., 2022: Scrutinizing tree-ring parameters for Holocene climate reconstructions. *Wiley Interdiscip. Rev.: Climate Change*, **13**, e778, https://doi.org/10.1002/wcc.778.

——, D. C. Frank, D. Nievergelt, and J. Esper, 2006: Summer temperature variations in the European Alps, A.D. 755–2004. *J. Climate*, **19**, 5606–5623, https://doi.org/10.1175/JCLI3917.1.

——, and Coauthors, 2011: 2500 years of European climate variability and human susceptibility. *Science*, **331**, 578–582, https://doi.org/10.1126/science.1197175.

——, and Coauthors, 2020: No age trends in oak stable isotopes. *Paleoceanogr. Paleoclimatol.*, **35**, e2019PA003831, https://doi.org/10.1029/2019PA003831.

——, and Coauthors, 2021: Recent European drought extremes beyond Common Era background variability. *Nat. Geosci.*, **14**, 190–196, https://doi.org/10.1038/s41561-021-00698-0.

Camenisch, C., and Coauthors, 2016: The 1430s: A cold period of extraordinary internal climate variability during the early Spörer minimum with social and economic impacts in northwestern and central Europe. *Climate Past*, **12**, 2107–2126, https://doi.org/10.5194/cp-12-2107-2016.

——, R. Brázdil, A. Kiss, C. Pfister, O. Wetter, C. Rohr, A. Contino, and D. Retsö, 2020: Extreme heat and drought in 1473 and their impacts in Europe in the context of the early 1470s. *Reg.*

Environ. Change, **20**, 19, https://doi.org/10.1007/s10113-020-01601-0.

Churakova-Sidorova, O. V., and Coauthors, 2022: Modern aridity in the Altai-Sayan mountain range derived from multiple millennial proxies. *Sci. Rep.*, **12**, 7752, https://doi.org/10.1038/s41598-022-11299-1.

Ciais, P., and Coauthors, 2005: Europe-wide reduction in primary productivity caused by the heat and drought in 2003. *Nature*, **437**, 529–533, https://doi.org/10.1038/nature03972.

Cook, E. R., and Coauthors, 2015: Old World megadroughts and pluvials during the Common Era. *Sci. Adv.*, **1**, e1500561, https://doi.org/10.1126/sciadv.1500561.

Esper, J., D. C. Frank, G. Battipaglia, U. Büntgen, C. Holert, K. Treydte, R. Siegfwolf, and M. Saurer, 2010: Low-frequency noise in $\delta^{13}C$ and $\delta^{18}O$ tree ring data: A case study of *Pinus uncinata* in the Spanish Pyrenees. *Global Biogeochem. Cycles*, **24**, GB4018, https://doi.org/10.1029/2010GB003772.

——, U. Büntgen, S. Denzer, P. J. Krusic, J. Luterbacher, R. Schäfer, R. Schreg, and J. Werner, 2017: Environmental drivers of historical grain price variations in Europe. *Climate Res.*, **72**, 39–52, https://doi.org/10.3354/cr01449.

——, and Coauthors, 2018: Site-specific climatic signals in stable isotope records from Swedish pine forests. *Trees*, **32**, 855–869, https://doi.org/10.1007/s00468-018-1678-z.

Farr, T. G., and Coauthors, 2007: The shuttle radar topography mission. *Rev. Geophys.*, **45**, RG2004, https://doi.org/10.1029/2005RG000183.

Fisher, R. A., 1921: On the 'probable error' coefficient of correlation deduced from a small sample. *Metron*, **1**, 3–32.

Fritts, H. C., 1976: *Tree Rings and Climate*. Academic Press, 582 pp.

Gessler, A., J. P. Ferrio, R. Hommer, K. Treydte, R. A. Werner, and R. K. Monson, 2014: Stable isotopes in tree rings: Towards a mechanistic understanding of isotope fractionation and mixing processes from the leaves to the wood. *Tree Physiol.*, **34**, 796–818, https://doi.org/10.1093/treephys/tpu040.

Gonsamo, A., and J. M. Chen, 2015: Winter teleconnections can predict the ensuing summer European crop productivity. *Proc. Natl. Acad. Sci. USA*, **112**, E2265–E2266, https://doi.org/10.1073/pnas.1503450112.

Hamed, K. H., and A. R. Rao, 1998: A modified Mann-Kendall trend test for autocorrelated data. *J. Hydrol.*, **204**, 182–196, https://doi.org/10.1016/S0022-1694(97)00125-X.

Harris, I., T. J. Osborn, P. Jones, and D. Lister, 2020: Version 4 of the CRU TS monthly high-resolution gridded multivariate climate dataset. *Sci. Data*, **7**, 109, https://doi.org/10.1038/s41597-020-0453-3.

Hartl-Meier, C., C. Zhang, U. Büntgen, J. Esper, A. Rothe, A. Göttlein, T. Dirnböck, and K. Treydte, 2015: Uniform climate sensitivity in tree-ring stable isotopes across species and sites in a mid-latitude temperate forest. *Tree Physiol.*, **35**, 4–15, https://doi.org/10.1093/treephys/tpu096.

Heim, R. R., Jr., 2002: A review of twentieth-century drought indices used in the United States. *Bull. Amer. Meteor. Soc.*, **83**, 1149–1166, https://doi.org/10.1175/1520-0477-83.8.1149.

Hlavinka, P., and Coauthors, 2011: Development and evaluation of the SoilClim model for water balance and soil climate estimates. *Agric. Water Manage.*, **98**, 1249–1261, https://doi.org/10.1016/j.agwat.2011.03.011.

Jordan, W. C., 1996: *The Great Famine: Northern Europe in the Early Fourteenth Century*. Princeton University Press, 317 pp.

Kendall, M. G., 1975: *Rank Correlation Methods*. 4th ed. Griffin Press, 202 pp.

Kern, Z., M. Patkó, M. Kázmér, J. Fekete, S. Kele, and Z. Pályi, 2013: Multiple tree-ring proxies (earlywood width, latewood width and δ^{13}C) from pedunculate oak (*Quercus robur* L.), Hungary. *Quat. Int.*, **293**, 257–267, https://doi.org/10.1016/j.quaint.2012.05.037.

Kiss, A., 2020: The great (1506–)1507 drought and its consequences in Hungary in a (central) European context. *Reg. Environ. Change*, **20**, 50, https://doi.org/10.1007/s10113-020-01634-5.

——, and Z. Nikolić, 2015: Droughts, dry spells and low water levels in medieval Hungary (and Croatia) I. *J. Environ. Geogr.*, **8**, 11–22, https://doi.org/10.1515/jengeo-2015-0002.

Leavitt, S. W., 2010: Tree-ring C–H–O isotope variability and sampling. *Sci. Total Environ.*, **408**, 5244–5253, https://doi.org/10.1016/j.scitotenv.2010.07.057.

Liu, Y., Y. Wang, Q. Li, H. Song, H. W. Linderholm, S. W. Leavitt, R. Wang, and Z. An, 2014: Tree-ring stable carbon isotope-based May–July temperature reconstruction over Nanwutai, China, for the past century and its record of 20th century warming. *Quat. Sci. Rev.*, **93**, 67–76, https://doi.org/10.1016/j.quascirev.2014.03.023.

Ljungqvist, F. C., P. Thejll, B. Christiansen, A. Seim, C. Hartl, and J. Esper, 2022: The significance of climate variability on early modern European grain prices. *Cliometrica*, **16**, 29–77, https://doi.org/10.1007/s11698-021-00224-7.

Luterbacher, J., and Coauthors, 2016: European summer temperatures since Roman times. *Environ. Res. Lett.*, **11**, 024001, https://doi.org/10.1088/1748-9326/11/2/024001.

McCarroll, D., and N. J. Loader, 2004: Stable isotopes in tree rings. *Quat. Sci. Rev.*, **23**, 771–801, https://doi.org/10.1016/j.quascirev.2003.06.017.

Mikšovský, J., R. Brázdil, M. Trnka, and P. Pišoft, 2019: Long-term variability of drought indices in the Czech Lands and effects of external forcings and large-scale climate variability. *Climate Past*, **15**, 827–847, https://doi.org/10.5194/cp-15-827-2019.

Mooney, C. Z., and R. D. Duval, 1993: *Bootstrapping: A Nonparametric Approach to Statistical Inference*. Sage University Paper Series on Quantitative Applications in the Social Sciences, Vol. 95, Sage Publications, 73 pp.

Moravec, V., Y. Markonis, O. Rakovec, M. Svoboda, M. Trnka, R. Kumar, and M. Hanel, 2021: Europe under multi-year droughts: How severe was the 2014–2018 drought period? *Environ. Res. Lett.*, **16**, 034062, https://doi.org/10.1088/1748-9326/abe828.

Možný, M., R. Brázdil, P. Dobrovolný, and M. Trnka, 2012: Cereal harvest dates in the Czech Republic between 1501 and 2008 as a proxy for March–June temperature reconstruction. *Climatic Change*, **110**, 801–821, https://doi.org/10.1007/s10584-011-0075-z.

——, and Coauthors, 2016: Drought reconstruction based on grape harvest dates for the Czech Lands, 1499–2012. *Climate Res.*, **70**, 119–132, https://doi.org/10.3354/cr01423.

Naumann, G., C. Cammalleri, L. Mentaschi, and L. Feyen, 2021: Increased economic drought impacts in Europe with anthropogenic warming. *Nat. Climate Change*, **11**, 485–491, https://doi.org/10.1038/s41558-021-01044-3.

Němec, J., 2001: *Assessment and Evaluation of Farm Land in the Czech Republic* (in Czech). Research Institute of Agriculture Economics, 257 pp.

Nguyen, H. T. T., S. Galelli, C. Xu, and B. Buckley, 2021: Multi-proxy, multi-season streamflow reconstruction with mass balance adjustment. *Water Resour. Res.*, **57**, e2020WR029394, https://doi.org/10.1029/2020WR029394.

Olive, D. J., 2007: Prediction intervals for regression models. *Comput. Stat. Data Anal.*, **51**, 3115–3122, https://doi.org/10.1016/j.csda.2006.02.006.

Palmer, W. C., 1965: Meteorological drought. U.S. Weather Bureau Research Paper 45, 58 pp., https://www.droughtmanagement.info/literature/USWB_Meteorological_Drought_1965.pdf.

Pauling, A., J. Luterbacher, C. Casty, and H. Wanner, 2006: Five hundred years of gridded high-resolution precipitation reconstructions over Europe and the connection to large-scale circulation. *Climate Dyn.*, **26**, 387–405, https://doi.org/10.1007/s00382-005-0090-8.

Pfister, C., and R. Brázdil, 2006: Social vulnerability to climate in the "Little Ice Age": An example from central Europe in the early 1770s. *Climate Past*, **2**, 115–129, https://doi.org/10.5194/cp-2-115-2006.

——, and H. Wanner, 2021: *Klima und Gesellschaft in Europa: Die letzten tausend Jahre.* Haupt Verlag, 424 pp.

Rybníček, M., T. Kolář, A. Ač, J. Balek, E. Koňasová, M. Trnka, O. Urban, and U. Büntgen, 2021: Non-pooled oak (*Quercus* spp.) stable isotopes reveal enhanced climate sensitivity compared to ring widths. *Climate Res.*, **83**, 27–41, https://doi.org/10.3354/cr01632.

Saurer, M., K. Aellen, and R. Siegwolf, 1997: Correlating δ^{13}C and δ^{18}O in cellulose of trees. *Plant Cell Environ.*, **20**, 1543–1550, https://doi.org/10.1046/j.1365-3040.1997.d01-53.x.

Schweingruber, F., and K. R. Briffa, 1996: Tree-ring density networks for climatic reconstruction. *Climatic Variations and Forcing Mechanisms of the Last 2000 Years*, P. D. Jones, R. S. Bradley, and J. Jouzel, Eds., NATO Series, Vol. **41**, Springer-Verlag, 44–66, https://doi.org/10.1007/978-3-642-61113-1_3.

Stahle, D. W., and Coauthors, 2020: Dynamics, variability, and change in seasonal precipitation reconstructions for North America. *J. Climate*, **33**, 3173–3195, https://doi.org/10.1175/JCLI-D-19-0270.1.

Štěpánek, P., P. Zahradníček, and P. Skalák, 2009: Data quality control and homogenization of air temperature and precipitation series in the area of the Czech Republic in the period 1961–2007. *Adv. Sci. Res.*, **3**, 23–26, https://doi.org/10.5194/asr-3-23-2009.

——, ——, and A. Farda, 2013: Experiences with data quality control and homogenization of daily records of various meteorological elements in the Czech Republic in the period 1961–2010. *Idojaras*, **117**, 123–141.

Tello, E., and Coauthors, 2017: The onset of the English agricultural revolution: Climate factors and soil nutrients. *J. Interdisc. Hist.*, **47**, 445–474, https://doi.org/10.1162/JINH_a_01050.

Treydte, K., and Coauthors, 2007: Signal strength and climate calibration of a European tree-ring isotope network. *Geophys. Res. Lett.*, **34**, L24302, https://doi.org/10.1029/2007GL031106.

——, D. C. Frank, M. Saurer, G. Helle, G. H. Schleser, and J. Esper, 2009: Impact of climate and CO_2 on a millennium-long tree-ring carbon isotope record. *Geochim. Cosmochim. Acta*, **73**, 4635–4647, https://doi.org/10.1016/j.gca.2009.05.057.

Trnka, M., and Coauthors, 2009a: Climate-driven changes of production regions in central Europe. *Plant Soil Environ.*, **55**, 257–266, https://doi.org/10.17221/1017-PSE.

——, J. Kyselý, M. Možný, and M. Dubrovský, 2009b: Changes in central-European soil-moisture availability and circulation patterns in 1881–2005. *Int. J. Climatol.*, **29**, 655–672, https://doi.org/10.1002/joc.1703.

——, and Coauthors, 2011a: Agroclimatic conditions in Europe under climate change. *Global Change Biol.*, **17**, 2298–2318, https://doi.org/10.1111/j.1365-2486.2011.02396.x.

——, and Coauthors, 2011b: A 200-year climate record in central Europe: Implications for agriculture. *Agron. Sustainable Dev.*, **31**, 631–641, https://doi.org/10.1007/s13593-011-0038-9.

——, R. P. Rötter, M. Ruiz-Ramos, K. C. Kersebaum, J. E. Olesen, Z. Žalud, and M. A. Semenov, 2014: Adverse weather conditions for European wheat production will become more frequent with climate change. *Nat. Climate Change*, **4**, 637–643, https://doi.org/10.1038/nclimate2242.

——, and Coauthors, 2021: Observed changes in the agroclimatic zones in the Czech Republic between 1961 and 2019. *Plant Soil Environ.*, **67**, 154–163, https://doi.org/10.17221/327/2020-PSE.

Urban, O., A. Ač, M. Rybníček, T. Kolář, N. Pernicová, E. Koňasová, M. Trnka, and U. Büntgen, 2021: The dendroclimatic value of oak stable isotopes. *Dendrochronologia*, **65**, 125804, https://doi.org/10.1016/j.dendro.2020.125804.

van der Schrier, G., K. R. Briffa, P. D. Jones, and T. J. Osborn, 2006: Summer moisture variability across Europe. *J. Climate*, **19**, 2818–2834, https://doi.org/10.1175/JCLI3734.1.

Voelker, S. L., F. C. Meinzer, B. Lachenbruch, J. R. Brooks, and R. P. Guyette, 2014: Drivers of radial growth and carbon isotope discrimination of buroak (*Quercus macrocarpa* Michx.) across continental gradients in precipitation, vapour pressure deficit and irradiance. *Plant Cell Environ.*, **37**, 766–779, https://doi.org/10.1111/pce.12196.

Wetter, O., and Coauthors, 2014: The year-long unprecedented European heat and drought of 1540—A worst case. *Climatic Change*, **125**, 349–363, https://doi.org/10.1007/s10584-014-1184-2.

Wilson, R. J. S., B. H. Luckman, and J. Esper, 2005: A 500 year dendroclimatic reconstruction of spring–summer precipitation from the lower Bavarian Forest region, Germany. *Int. J. Climatol.*, **25**, 611–630, https://doi.org/10.1002/joc.1150.